The International Maritime Transport and Logistics (MARLOG 13) - ISSN 2974-3141
http://dx.doi.org/10.21622/MARLOG.2024.13.1.101
Towards Smart Green Blue Infrastructure

Numerical analysis of enhancing water-drop fairing design to mitigate vortex-induced vibrations by applying angular slot

Michael Adel Shafik [1,2], Mina G. Mourad [2], Osama E. Abdellatif [2] and Ahmed S. Shehata [3]

(1) Basic and Applied Science Department, College of Engineering and Technology, Arab Academy for Science Technology and Maritime Transport, P.O. 1029 Aboukir, Alexandria, Egypt, michael.adel@aast.edu
(2) Mechanical Engineering Department, Shoubra Faculty of Engineering, Benha University, 108 Shoubra Street, Cairo, Egypt, mina.morad@feng.bu.edu.eg
(3) Mechanical Engineering Department, Shoubra Faculty of Engineering, Benha University, 108 Shoubra Street, Cairo, Egypt, osama.abdellatif@feng.bu.edu.eg
(4) Marine Engineering Department, College of Engineering and Technology, Arab Academy for Science Technology and Maritime Transport, P.O. 1029 Aboukir, Alexandria, Egypt, a_samir@aast.edu

Keywords: Marine riser, vortex-induced vibration, CFD

1. **ABSTRACT:** Marine risers are crucial components of offshore oil and gas production systems, connecting the seabed to the surface platform. They are susceptible to vortex-induced vibrations (VIV). As a result, marine risers are susceptible to failure, which can have disastrous effects, including environmental damage, loss of output, and even loss of life. Vortices that are generated in the viscous boundary layer tend to separate toward the downstream end of the cylinder. A fairing is a body with a hydrofoil shape added to the marine risers to reduce the effect of VIV on the marine riser. The investigation will be undertaken using a two-dimensional computational Fluid dynamics model using the software ANSYS Fluent. A slot is applied to a water-drop fairing that has a top shape angle of 80° to improve the suppression of the VIV. The behavior of the fairing in VIV is compared using the root mean square of the lift coefficient ($C_{l\,RMS}$). The angle between the slot and the vertical is altered to discover the ideal angle that shows the lowest value of $C_{l\,RMS}$. The results of the current investigation identified the ideal possible angle for the slot. The slot that has an angle of 30 clockwise with vertical has been shown to be the best at dampening VIV, with a 37.8% reduction in $C_{l\,RMS}$.

2. INTRODUCTION

Floating offshore structures are crucial for harvesting energy and resources from the sea, giving diverse platforms for oil drilling, wind farms, and more. Central to their performance is the marine riser, a crucial component that connects the bottom equipment to the surface facilities, enabling the transfer of substances like oil and gas. However, the potential of VIV poses a serious obstacle to modern maritime risers. VIV develops when currents interact with the riser, generating oscillations that can lead to fatigue and structural damage. This not only undermines the integrity of the riser itself but also jeopardizes the stability and safety of the entire floating offshore structure, underscoring the significance of finding ways to decrease VIV and assure the reliability of these vital marine systems. Wang et al.[1] numerically explored circular cylinder wake control by a fairing with a Total Variation Diminishing – Finite Volume Method (TVD–FVM) approach. The mechanism of vortex shedding suppression is described and may be well explained by the formation length of tail vortices, which correlates to the suction pressure coefficient and turbulent kinetic. Chen et al. [2] employed a genetic algorithm to identify the optimum design of two-dimensional riser fairings to

decrease the VIV. Janardhanan [3] computed the efficacy of the fairing arrangement in lowering the VIV of the matching bluff body. Liu et al. [4] proposes a new 2D model for analysing VIV in circular cylinders, confirmed by precise simulation of high-Reynolds VIV versus existing data. The major findings demonstrate how cylinder mass ratio effects VIV behaviour: low mass cylinders (m* = 0.7) experience irregular vortex shedding and greater vibration amplitudes, while high mass cylinders (m* = 2.4) exhibit regular shedding and lower vibration. They conclude that the mass ratio has a great effect on the fluid force and the vibration amplitude, especially in the "locking" region for the circular cylinder with a mass ratio of less than 1.0. A comparison is done by Zheng and Wang [5]between water-drop and short-tail-shaped fairings to investigate the galloping oscillations. They conclude that both fairings have equal galloping performances under various reduced velocities when they have the same characteristic lengths. Zheng and Wang [6] studied the numerical study of galloping oscillation of a two-dimensional circular cylinder with a fairing, emphasizing the significance of predicting such oscillations to prevent structural failures. Also, LIU et al. [7] presents a novel approach by investigating the control of VIV using numerous rods at low Reynolds numbers. Their model demonstrates that the use of short, closely positioned rods significantly decreases cylinder vibration. studying the dynamics of multi-cylinder VIV can gain a more comprehensive understanding of this phenomenon. Xu et al. [8] investigate the challenges of predicting VIV of an inclined flexible cylinder using traditional methods and proposes machine learning as an alternative.

The authors establish prediction models using three different algorithms and find that support vector machine (SVM) is the most suitable for this application. Wu et al. [9]study addresses controlling VIV in pipeline plugging procedures, vital for pipeline maintenance. The authors offer a unique technique using varied end face forms, plugging rates, and spoiler devices. Their findings suggest hemispherical end faces and greater plugging speeds to be the most effective, with active spoiler devices adding further attenuation. This research paves the door for safer and more dependable pipeline plugging. Song et al. [10] describes a method for managing VIV in a single cylinder using the Linear Quadratic Regulator (LQR) method. The efficiency of the strategy is verified through theoretical modelling, numerical analysis, and comparison with existing studies. The study demonstrates that the LQR approach can efficiently suppress VIV throughout a range of Reynolds numbers and control parameters. Boersma et al. [11] investigates the suppression of VIV of a cylinder in inertial-elastic flow. The authors explore the influence of adding elasticity to the fluid on the VIV response. Their findings reveal that adding elasticity can not only reduce the amplitude of oscillations but also completely suppress VIV. Additionally, they observe a delay in the onset of VIV with increasing fluid elasticity. The wakes of the cylinders in the viscoelastic fluids deviate from those in Newtonian fluids, exhibiting more elongated vortices with tails. Wu et al. [12] study demonstrates three approaches to reduce subsea pipeline vibration: hemispherical end faces, slower plugging speeds, and smart spoiler positioning. Each decreases pressure variations and vortex shedding, ultimately safeguarding the pipeline. More complex sea conditions need exploration to ensure real-world effectiveness. Tao et al. [13] article provides a new model for forecasting VIV in cylinders near walls. It evaluates how the spacing between the cylinder and the wall, together with the flow speed, affect the forces acting on the cylinder. The model analyses elements such the Strouhal number, which links the cylinder size, flow speed, and vortex shedding frequency. It also accounts for changes in lift forces related to the gap size. Jang et al. [14] article provides a new method for forecasting fatigue damage in ship rudders due by VIV.

Traditional methods have limitations; thus, the authors developed an orthonormal modal fluid-structure interaction (FSI) analytical approach. They validated their method on a hydrofoil model and then applied it to a real ship rudder. The results show that the new technique accurately predicts fatigue characteristics, making it a significant tool for improving ship rudder design and decreasing maintenance costs. Shehata et al. [15] calculated that with the use of passive flow control, the torque coefficient of the blade increases by more than 40% within the stall regime and by more than 17% before the stall happens. Shehata et al. [16] Shehata et al. [17] evaluated the effect of

adjusting the slot angle on the Wells turbine's performance in the stall regime. Based on real data from Egypt's Northern Coast, the Oscillating Water Column (OWC) was utilized to investigate the blade of a turbine with an optimal hole angle. The optimal hole angle was identified to be 10° clockwise, which resulted in a 3% increase in torque coefficient before the stall and a 15% increase after the stall when compared to the 0° hole. Shehata et al. [18] used the multi-suction holes as passive flow control. Two, three, and four suction holes were studied to increase the performance of the wells' turbines in the stall regime. It is observed that the aerofoil with three suction holes situated at 40%, 55%, and 90% of the leading edge in chord percentage produces the maximum torque coefficient of 26.7% before the stall and 51% after the stall.

The fairing with a top shape angle θ of 80° stands out as the least favourable among its counterparts with angles of 20°, 40°, and 60° when evaluating its susceptibility to VIV [19]. However, despite this shortcoming, it has a major advantage due to its reduced chord length. This decreased length equates to a more cheap and practical solution compared to the other fairings. To boost the efficiency of the 80° top angle fairing in decreasing VIV, perfecting its design becomes vital. By fine-tuning its structural features or making improvements intended at minimizing vortex-induced vibrations, it can potentially improve its performance while keeping the cost-effectiveness obtained from its decreased chord length.

3. METHODOLOGY

In a prior study [19] a vertical slot was implemented on a fairing with an angle of θ = 80° at multiple locations to enhance the fairing's capacity to dampen vortex-induced vibrations. The point 0.13D was determined to be the optimal position, as it exhibits the lowest value for $C_{l\,RMS}$. In this work, an angled slot is implemented at the identical position of 0.13D to enhance the fairing's capability to reduce vortex-induced vibrations. A two-dimensional computational domain was utilized to match the flow patterns over these water-drop arrays, displayed in Figure 1 aligned with the direction of the streamflow. The computational domain design tries to ensure that boundary limits do not alter the numerical predictions of the flow fields. It extends 5D upstream and 30D downstream of the fairing, with inlet and outflow borders fixed at a width of 10D, the value of D is assigned as 1 meter. At the inlet, a longitudinally uniform velocity 1m/s, corresponding to $Re = 10^6$, is introduced, establishing the inlet boundary condition as a velocity inlet. The outlet boundary condition is established as a pressure outlet. Symmetry boundary conditions are applied to the upper and lower walls, while the fairing's walls are subjected to a no-slip boundary condition.

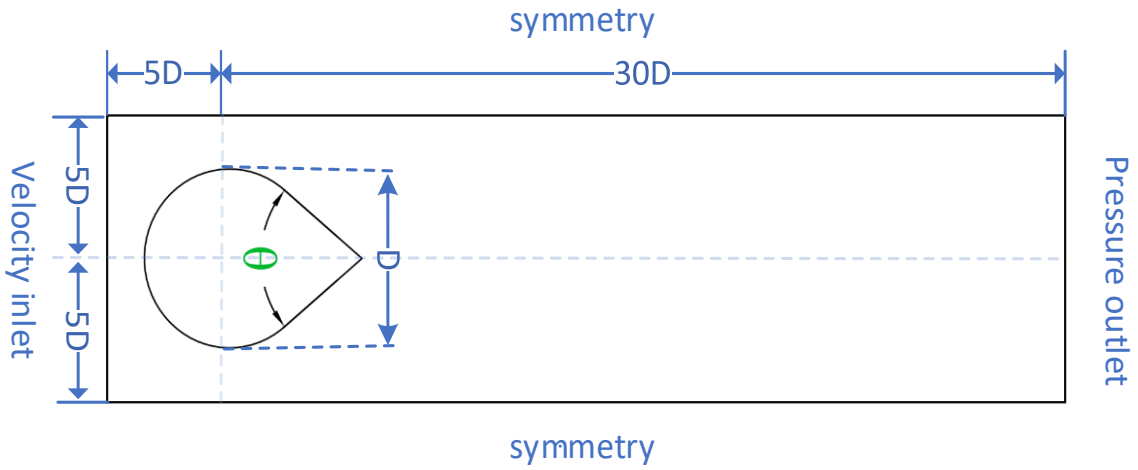

Figure 1 simulation domain and boundary conditions of a water-drop fairing that have a top shape angle θ

The numerical simulation is performed using SST k-ω turbulence model. The SST k-ω turbulence model uses the traditional k-ω model near the wall, which accurately replicates laminar flow with a reverse pressure gradient on the fairing surface. When dealing with the flow away from the wall, however, it uses the normal k-ε model. The SST k-ω model's governing equations are based on the turbulence kinetic energy (k) and the turbulence-specific dissipation rate (ω).

For turbulence kinetic energy (k):

$$\frac{D}{Dt}(\rho k) = \nabla \cdot (\rho D_k \nabla k) + \rho G - \frac{2}{3}\rho k(\nabla \cdot \mathbf{u}) - \rho \beta^* \omega k + S_k \quad (1)$$

For turbulence specific dissipation rate (ω):

$$\frac{D}{Dt}(\rho \omega) = \nabla \cdot (\rho D_k \nabla \omega) + \frac{\rho \gamma G}{\nu} - \frac{2}{3}\rho \gamma \omega(\nabla \cdot u) - \rho \beta \omega^2 - \rho(F_1 - 1)CD_{k\omega} + S_\omega \quad (2)$$

Turbulence viscosity:

$$\nu_t = a_1 \frac{k}{\max(a_1, \omega, b_1, F_{23})} \quad (3)$$

The simulation model was run on a PC with a CPU Intel® Core™ i7-12700 and 32 GB ram using ANSYS fluent software. In order to obtain the densest possible mesh, a total of 873154 elements are utilized, with each element having a minimum size of 0.02 mm, which is the smallest size that the PC is capable of handling. Erroneous mesh values can undermine research, leading to misleading conclusions. To verify and confirm the accuracy of the turbulence model employed in this study, the drag coefficient value is compared to data published by Hoerner's experimental data[20] that indicate that the drag coefficient for a fairing with a top shape angle of 80 at Reynolds number 10^6 is 0.18229. White [21] reprinted the data in Fluid Textbook. The simulation is in good agreement with Hoerner's results, with a drag coefficient of 0.19070 and a percentage error of 4.62%.

Figure 2 summarizes the methodology process in a flowchart diagram. Start: The process begins with a user-defined geometry for a fairing with an angled slot. Change for each angle: the simulation is run for numerous angles of the slot. to understand how the VIV responds with each angle. Mesh creation: The following step is to generate a mesh around the shape. Pre-processor: The data is prepared for the solver during the pre-processor step. Solver: The solver is at the heart of the CFD simulation. It calculates the fluid flow at each location in the mesh using the mesh and the boundary conditions. Results: The results of the simulation are typically stored in a file that can be visualized and analyzed. The desired results are the drag and lift coefficients of the fairing. Post-processor: The post-processor is used to visualize and analyze the results of the simulation. Ansys post-processing tools were used to create representations of the data. Data analysis: The final step in the process is to analyze the results of the simulation. This involves comparing the results to previous data of a vertical slot to improve the performance of the fairing to supress VIV.

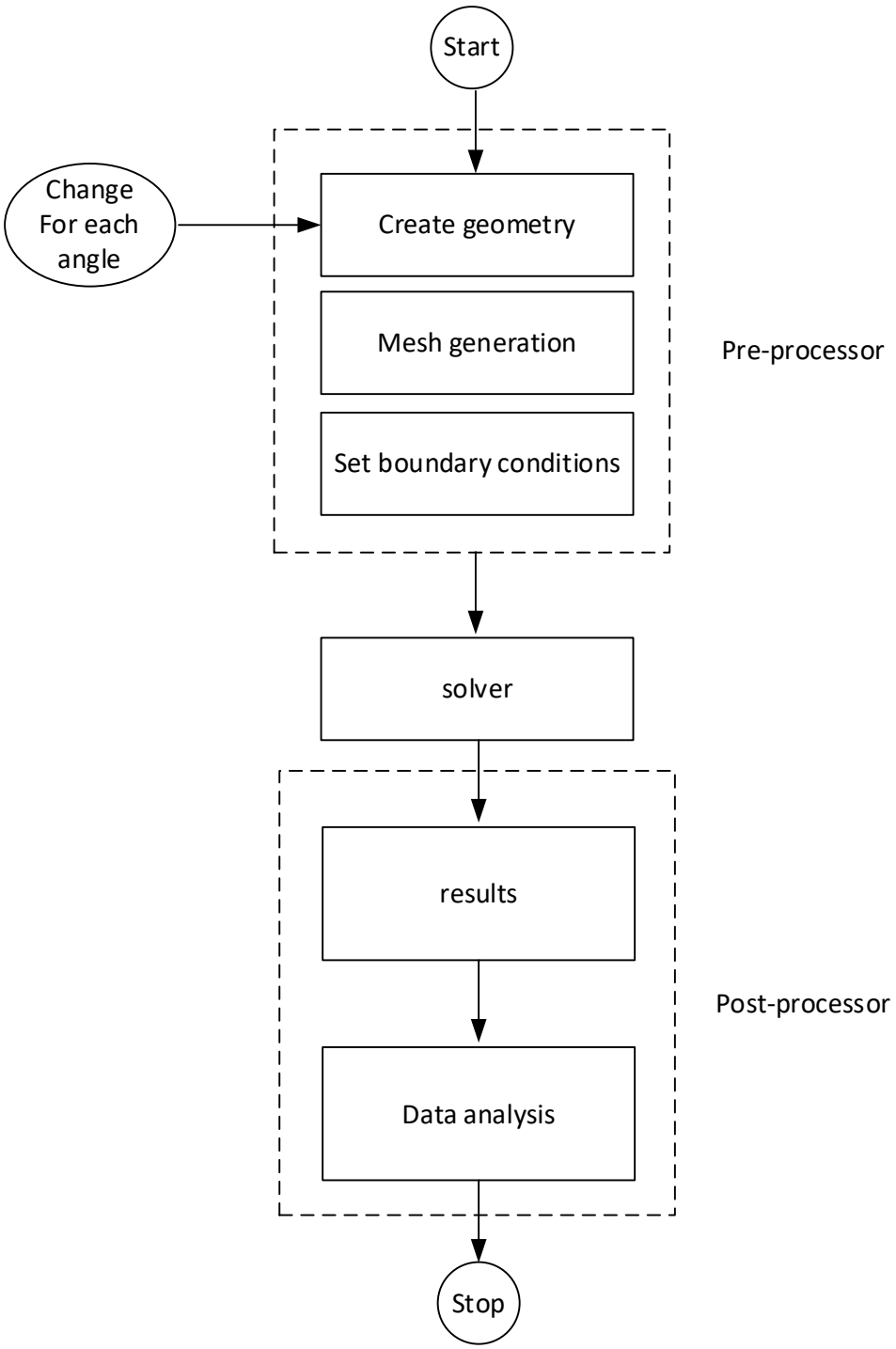

Figure 2 flowchart of research methodology

4. RESULTS & DISCUSSION

A vertical slot with a diameter of 0.01D was applied at the position 0.13D from the end of the fairing. The position is chosen according to previous research [19] as it proves to be the ideal position to apply a vertical slot on this fairing. The angle β is either measured clockwise β_{cw} or counterclockwise β_{ccw} . the angle is increased from 0 to 40 in both directions with a step size of 5 as shown in figure 3.The slot with an angle β equals 30 cw is the best in dampening VIV as its decreases the value of $C_{I\,RMS}$ by 37.8%, also the slots with an angle β equals 15 ccw and 5 cw is the

fair as they show a decrease in $C_{l\,RMS}$ by 9.38 % and 6.11 % respectively compared to the vertical slot.

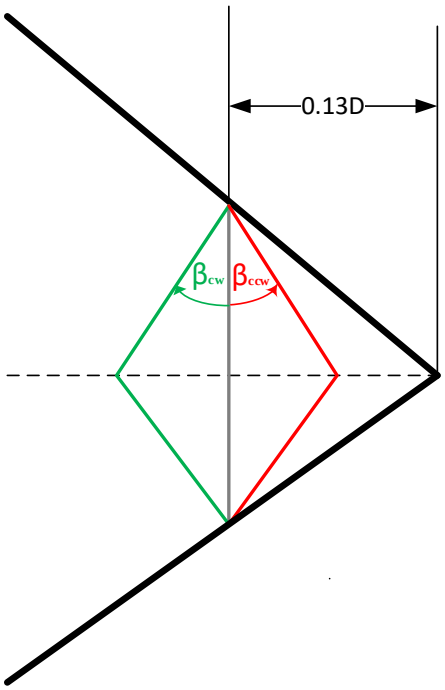

Figure 3 Angled slot applied at 0.13D from the end of water-drop fairing.

Table 1 displays the C_d, C_l and $C_{l\,RMS}$ values for the water-drop fairing with a clockwise inclined slot β_{cw}.Figure 4 shows the root mean square (RMS) values of the C_l (lift coefficient) values for the water-drop fairing with clockwise angled slot β_{cw}. for the water-drop fairing with a clockwise angled slot β_{cw}.

Table 1 C_d, C_l, and $C_{l\,RMS}$ for a water-drop fairing with clockwise angled slot

		% increase		% increase
β_{cw}	C_d	or decrease	$C_{l\,RMS}$	or decrease
0	0.1624	Datum	0.0702	datum
5	0.1203	-25.94	0.0659	-6.11
10	0.1193	-26.52	0.1724	145.50
15	0.1223	-24.72	0.1631	132.27
20	0.1149	-29.21	0.1567	123.19
25	0.1296	-20.18	0.5543	689.41
30	0.1203	-25.95	0.0437	-37.83
35	0.1160	-28.58	0.1656	135.84
40	0.1233	-24.06	0.1370	95.19

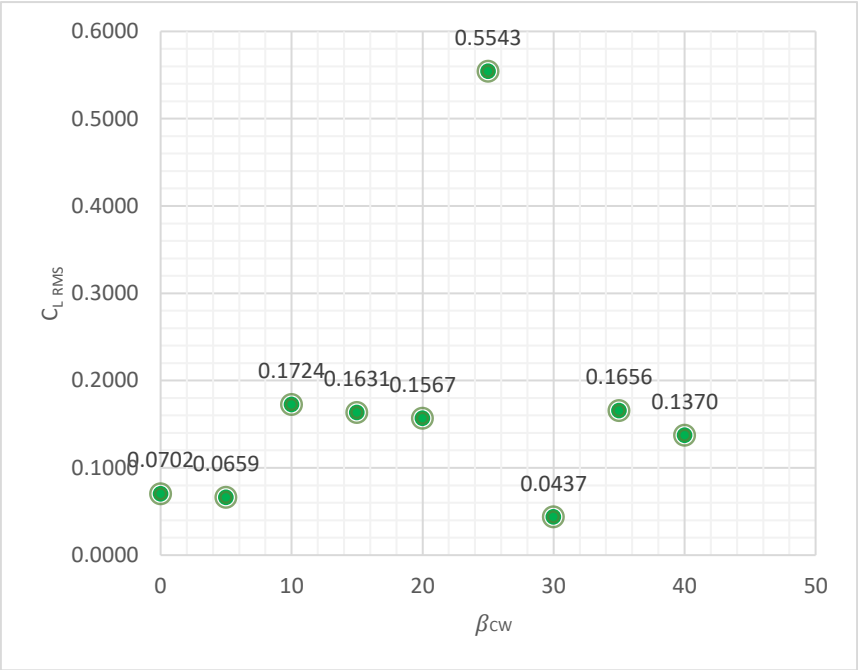

Figure 4 $C_{l\,RMS}$ for a water-drop fairing with clockwise angled slot β_{cw}

Table 2 displays the C_d, C_l and $C_{l\,RMS}$ values for the water-drop fairing with a counterclockwise inclined slot β_{cw}.Figure 5 shows the root mean square (RMS) values of the C_l (lift coefficient) values for the water-drop fairing with counterclockwise angled slot β_{ccw}. for the water-drop fairing with a clockwise angled slot β_{ccw}.

Table 2 C_d , C_l , and $C_{l\,RMS}$ for a water-drop fairing with counterclockwise angled slot

		% increase		%increase
β_{ccw}	C_d	or decrease	$C_{l\,RMS}$	or decrease
0	0.1624	datum	0.0702	datum
5	0.1625	0.06	0.1548	120.49
10	0.1615	-0.56	0.0706	0.62
15	0.1620	-0.23	0.0636	-9.38
20	0.1755	8.08	0.2865	308.06
25	0.1066	-34.36	0.1483	111.24
30	0.1599	-1.53	0.1773	152.54
35	0.1584	-2.44	0.1163	65.68
40	0.1880	15.76	0.1724	145.50

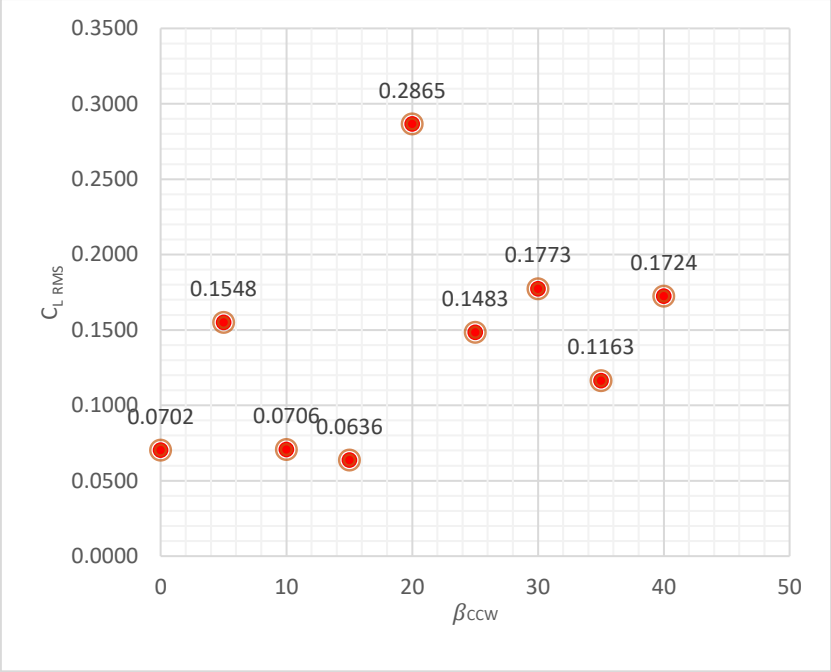

Figure 5 $C_{l\,RMS}$ for a water-drop fairing with counterclockwise angled slot β_{ccw}

The velocity streamline visualization shown in figure 6 reveals that the flow boundary layer detaches later for angled slot fairings in comparison to the vertical slot. The delayed separation observed suggests enhanced flow adherence and decreased pressure fluctuations, perhaps resulting in reduced VIV amplitudes.

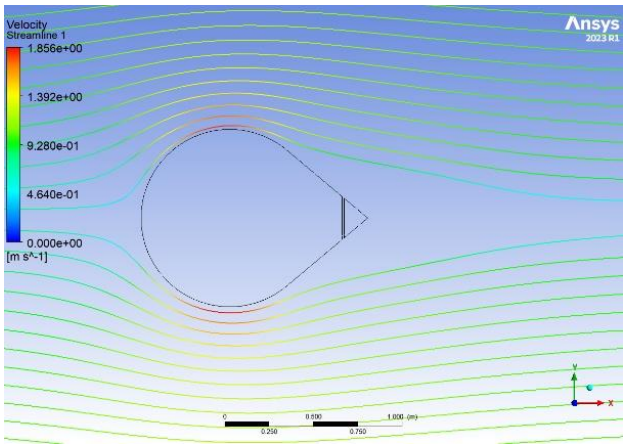

vertical slot

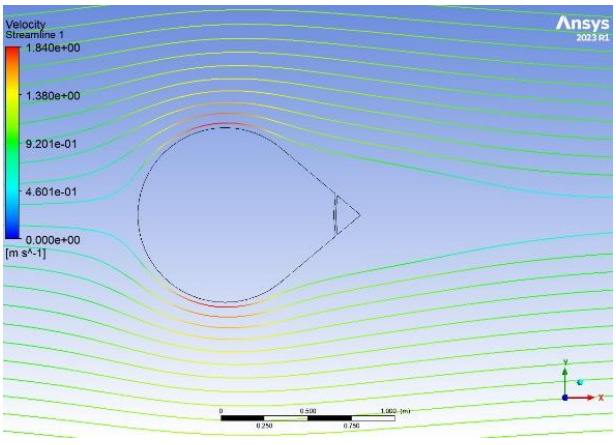

$\beta = 5°\ cw$

The International Maritime Transport and Logistics (MARLOG 13) - ISSN 2974-3141
http://dx.doi.org/10.21622/MARLOG.2024.13.1.101
Towards Smart Green Blue Infrastructure

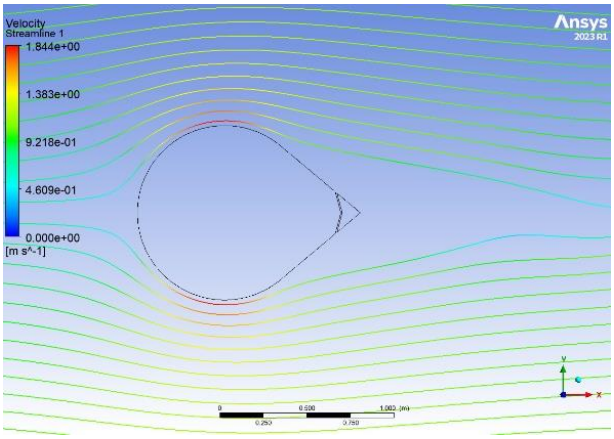

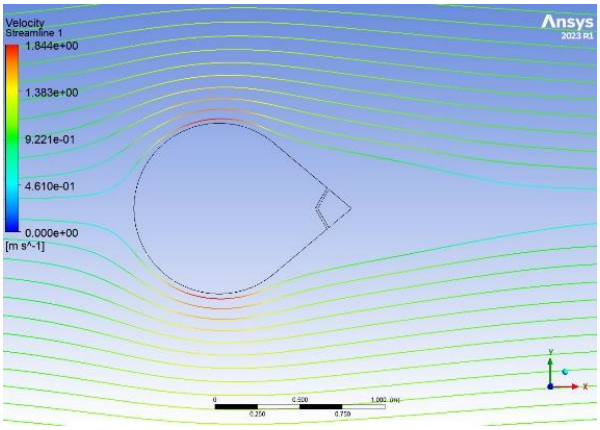

$\beta = 15° \; ccw$ $\beta = 30° \; cw$

Figure 6 velocity streamline for different angled slot fairing

The comparison of pressure contours shown in figure 7 clearly demonstrates a noticeable change in the wake area when using angled slot fairings as opposed to vertical slot. The observed change suggests a disturbance in the regular patterns of vortex shedding, which could result in a decrease in VIV as anticipated by the flow models.

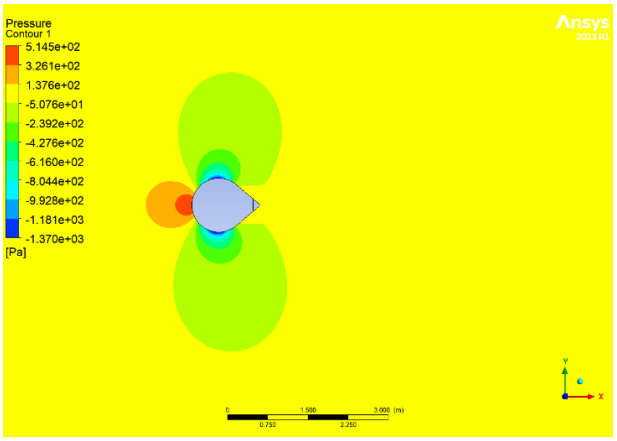

vertical slot

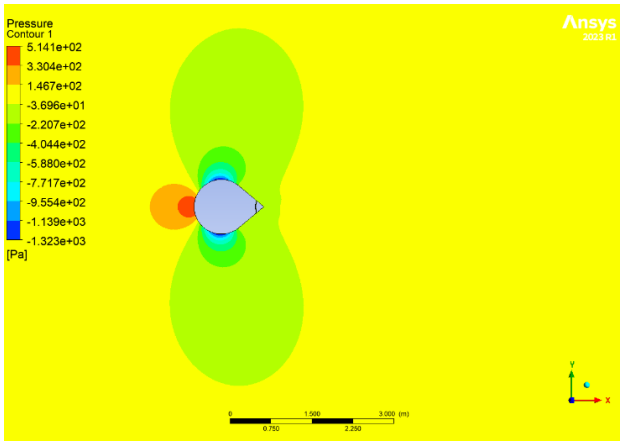

$\beta = 5° \; cw$

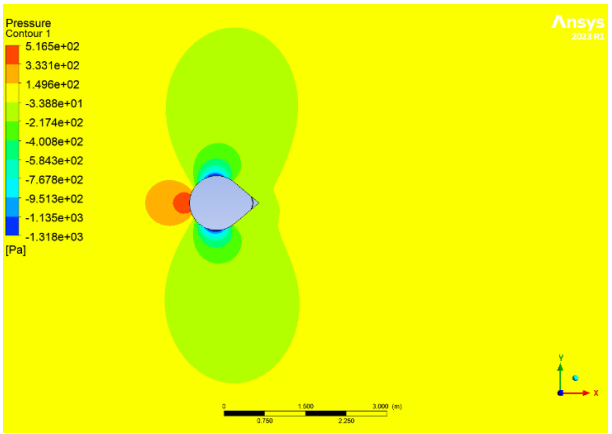

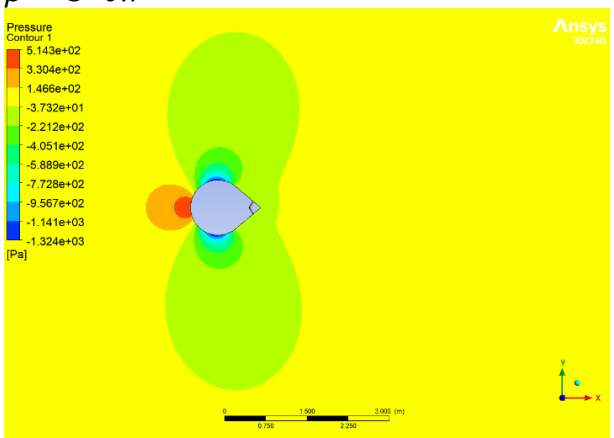

$\beta = 15° \; ccw$ $\beta = 30° \; cw$

Figure 7 pressure contours for different angled slot fairing

Figure 8 shows that angled slot fairings demonstrate a noticeably lower overall level of Turbulence kinetic energy compared to the vertical slot, signifying a decrease in the overall energy associated

with turbulent fluctuations. This suggests a calmer flow regime and potentially reduced energy transfer to the cylinder, leading to lower VIV response.

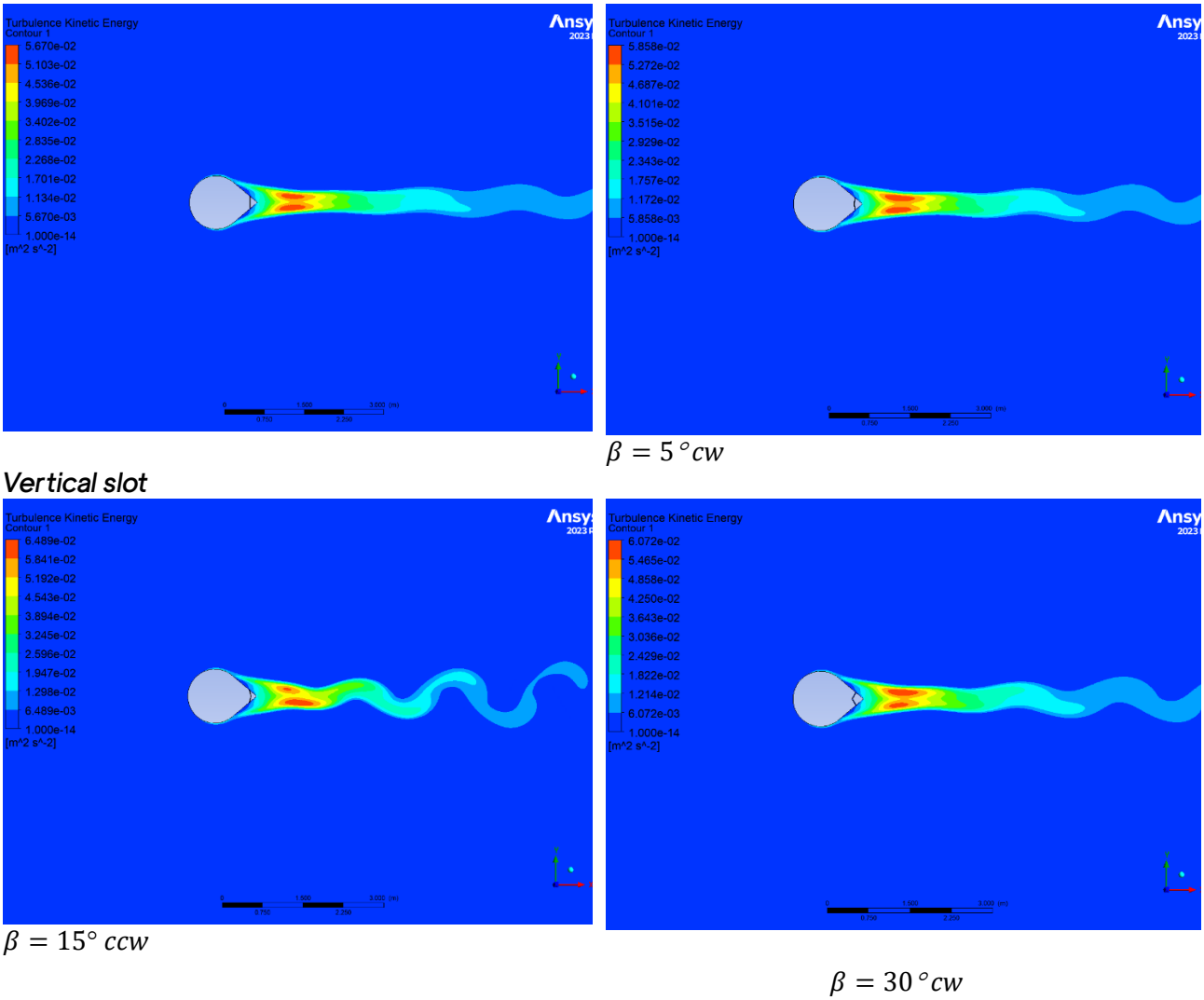

Figure 8 Instantaneous turbulent kinetic contours for different angled slot fairing

5. CONCLUSION

A vertical slot with a diameter of 0.01D was applied at the position 0.13D from the end of the fairing. The fairing with an angle β equals 30 cw with vertical has proved to be the best in damping VIV as its results show the lowest value of $C_{l\ RMS}$. it shows a decrease of 37.8%. additionally, the slots with an angle β = 15 ccw and 5 cw is the fair as they exhibit a drop in $C_{l\ RMS}$ by 9.38 % and 6.11 % respectively compared to the vertical slot. Future work should focus on using a structured mesh as it speeds computation time. utilizing a three-dimensional model presents different optimization situations, unlocking alternatives through its additional dimension. Furthermore, study various dimensions and numbers of holes to be applied on the fairings to acquire better outcomes to reduce VIV.

6. REFERENCES

[1] J. Wang, H. Zheng, and Z. Tian, "Numerical simulation with a TVD-FVM method for circular cylinder wake control by a fairing," *J Fluids Struct*, vol. 57, pp. 15–31, Aug. 2015, doi: 10.1016/J.JFLUIDSTRUCTS.2015.05.008.

[2] M. Chen, X. Liu, F. Liu, and M. Lou, "Optimal design of two-dimensional riser fairings for vortex-induced vibration suppression based on genetic algorithm," *arXiv: Fluid Dynamics*, 2018, [Online]. Available: https://api.semanticscholar.org/CorpusID:119040921

[3] A. Janardhanan, "Reducing Vortex-Induced Vibration of Drilling Risers with Marine Fairing," 2014. [Online]. Available: https://api.semanticscholar.org/CorpusID:108047055

[4] M. Liu, R. Jin, and H. Wang, "Numerical investigation of vortex induced vibration of a circular cylinder for mass ratio less than 1.0," *Ocean Engineering*, vol. 251, p. 111130, May 2022, doi: 10.1016/J.OCEANENG.2022.111130.

[5] H. Zheng and J. Wang, "Galloping oscillation of a circular cylinder firmly combined with different shaped fairing devices," *J Fluids Struct*, vol. 77, pp. 182–195, Feb. 2018, doi: 10.1016/J.JFLUIDSTRUCTS.2017.12.010.

[6] H. Zheng and J. Wang, "Numerical study of galloping oscillation of a two-dimensional circular cylinder attached with fixed fairing device," *Ocean Engineering*, vol. 130, pp. 274–283, Jan. 2017, doi: 10.1016/J.OCEANENG.2016.11.074.

[7] M.-M. LIU, H.-C. WANG, F.-F. SHAO, X. JIN, G.-Q. Tang, and F. YANG, "Numerical investigation on vortex-induced vibration of an elastically mounted circular cylinder with multiple control rods at low Reynolds number," *Applied Ocean Research*, vol. 118, p. 102987, 2022, doi: https://doi.org/10.1016/j.apor.2021.102987.

[8] W. Xu, Z. He, L. Zhai, and E. Wang, "Vortex-induced vibration prediction of an inclined flexible cylinder based on machine learning methods," *Ocean Engineering*, vol. 282, p. 114956, 2023, doi: https://doi.org/10.1016/j.oceaneng.2023.114956.

[9] T. Wu, X. Miao, H. Zhao, L. Wang, L. Li, and S. Li, "Experimental research on vortex-induced vibration suppression of pipeline intelligent plugging operation," *Eng Fail Anal*, vol. 157, p. 107868, 2024, doi: https://doi.org/10.1016/j.engfailanal.2023.107868.

[10] J. Song, J. Du, and Y. Yao, "Applying LQR to control cross vortex-induced vibration of cylinders based on wake oscillators," *Ocean Engineering*, vol. 286, p. 115631, 2023, doi: https://doi.org/10.1016/j.oceaneng.2023.115631.

[11] P. R. Boersma, J. P. Rothstein, and Y. Modarres-Sadeghi, "Suppression of vortex-induced vibrations of a cylinder in inertial-elastic flow," *J Nonnewton Fluid Mech*, vol. 324, p. 105170, 2024, doi: https://doi.org/10.1016/j.jnnfm.2023.105170.

[12] T. Wu, X. Miao, H. Zhao, L. Wang, L. Li, and S. Li, "Experimental research on vortex-induced vibration suppression of pipeline intelligent plugging operation," *Eng Fail Anal*, vol. 157, p. 107868, 2024, doi: https://doi.org/10.1016/j.engfailanal.2023.107868.

[13] M.-M. Tao, X. Sun, J. Xiao, and Y. Shu, "A novel vortex-induced vibration model for a circular cylinder in the vicinity of a plane wall," *Ocean Engineering*, vol. 287, p. 115846, 2023, doi: https://doi.org/10.1016/j.oceaneng.2023.115846.

[14] W.-S. Jang, W.-S. Choi, H.-G. Choi, S.-Y. Hong, and J.-H. Song, "Fatigue damage prediction of ship rudders under vortex-induced vibration using orthonormal modal FSI analysis," *Marine Structures*, vol. 88, p. 103376, 2023, doi: https://doi.org/10.1016/j.marstruc.2023.103376.

[15] A. S. Shehata, Q. Xiao, K. M. Saqr, A. Naguib, and D. Alexander, "Passive flow control for aerodynamic performance enhancement of airfoil with its application in Wells turbine – Under oscillating flow condition," *Ocean Engineering*, vol. 136, pp. 31–53, May 2017, doi: 10.1016/J.OCEANENG.2017.03.010.

[16] A. S. Shehata, Q. Xiao, M. A. Kotb, M. M. Selim, A. H. Elbatran, and D. Alexander, "Effect of passive flow control on the aerodynamic performance, entropy generation and aeroacoustic noise of axial turbines for wave energy extractor," *Ocean Engineering*, vol. 157, pp. 262–300, 2018, doi: https://doi.org/10.1016/j.oceaneng.2018.03.053.

[17] A. Shehata, "Investigation and improvement of Wells turbine performance : fluid analysis & 2nd law of thermodynamics study," 2017.

[18] A. S. Shehata, Q. Xiao, M. M. Selim, A. H. Elbatran, and D. Alexander, "Enhancement of performance of wave turbine during stall using passive flow control: First and second law analysis," *Renew Energy*, vol. 113, pp. 369–392, Dec. 2017, doi: 10.1016/J.RENENE.2017.06.008.

[19] M. A. Shafik, M. G. Mourad, A. S. Shehata, and O. E. Abdellatif, "Numerical study of vortex induced vibration of a two-dimensional circular cylinder attached with water-drop fairing with a vertical hole," in *AIP Conference Proceedings*, AIP Publishing, 2023. doi: https://doi.org/10.1063/5.0129334.

[20] S. F. Hoerner, *Fluid-Dynamic Drag: Theoretical, Experimental and Statistical Information*. Hoerner Fluid Dynamics, 1965. [Online]. Available: https://books.google.com.eg/books?id=cJs0mwEACAAJ

[21] F. M. White, "Fluid Mechanics, McGraw-Hill New York," in *McGraw-Hill*, 2003.